Hindawi
Advances in Civil Engineering
Volume 2024, Article ID 6651094, 14 pages
https://doi.org/10.1155/2024/6651094

Research Article

Bone Char Adsorption of COD and Colour from Tannery Wastewater: Breakthrough Curve Analysis and Fixed Bed Dynamic Modelling

Miriam Appiah-Brempong,[1] **Helen Michelle Korkor Essandoh**,[1] **Nana Yaw Asiedu**,[2] **and Francis Yao Momade**[3]

[1]*Regional Water and Environmental Sanitation Centre Kumasi, Department of Civil Engineering, College of Engineering, Kwame Nkrumah University of Science and Technology, Kumasi, Ghana*
[2]*Department of Chemical Engineering, College of Engineering, Kwame Nkrumah University of Science and Technology, Kumasi, Ghana*
[3]*Department of Materials Engineering, College of Engineering, Kwame Nkrumah University of Science and Technology, Kumasi, Ghana*

Correspondence should be addressed to Miriam Appiah-Brempong; esisamiriam@yahoo.co.uk

Received 16 October 2023; Revised 6 December 2023; Accepted 7 February 2024; Published 20 February 2024

Academic Editor: Loke Kok Foong

This study delves into the simultaneous adsorption of chemical oxygen demand (COD) and colour from tannery wastewater using bone char through a fixed bed column. The bone char, which was derived from cattle skulls, was characterised using the Fourier transform infrared spectroscopy, Braeuer–Emmett–Teller surface area analysis, and the scanning electron microscope/energy-dispersive X-ray spectroscopy. The effects of different process conditions, specifically, packed bed height (5, 10, and 15 cm) and flow rate (2, 5, and 8 mL/min), on the adsorption efficiency of the fixed bed column were assessed through breakthrough curve analysis. The results revealed that the efficiency of the column bed enhanced with increasing bed height and declined with increasing wastewater flow rate. The optimal operating conditions for COD and colour removal onto the bone char occurred at 15 cm bed height and 2 mL/min flow rate. The adsorption capacities at these conditions were 227.4 mg/g and 53.03 Pt-Co/g for COD and colour, respectively. The kinetics associated with the fixed bed adsorption of COD and colour onto bone char were elucidated through the fitting of the Thomas, Adams–Bohart, and Yoon–Nelson models to the experimental data. Among the three models, the Yoon–Nelson model gave the best prediction of the experimental data. Maximum adsorption efficiencies of 80.65% and 84% were attained for COD and colour removal, respectively, proving that bone char is a promising and ecologically friendly alternative adsorbent for the treatment of tannery wastewater.

1. Introduction

Tanneries are numbered among the most polluting industries in the world [1]. The utilisation of diverse chemicals, including dyes, chromium salt, aldehydes, vegetable tannins, bactericides, sodium chloride, surfactants, sodium sulphide, sulphonated oils, lime, ammonium sulphate, sulphuric, and formic acids [2, 3] coupled with hair, blood, and flesh, which exude from the animal skins or hides results in very highly complex and toxic wastewater [4]. Not only is this wastewater strongly odourous, saline, and coloured, but it is also heavily laden with suspended matter, nitrogenous substances, and recalcitrant organic matter, which is usually measured as chemical oxygen demand (COD) [5]. Worrisomely, this noxious wastewater is often indiscriminately discharged into rivers and lakes, particularly in low-income countries, including Bangladesh [6], Nigeria [7], Ethiopia [8], Ghana [9], and Pakistan [10]. This practice has a deleterious impact on both humans and the

environment, resulting in the destruction of surface and underground water quality, loss of biodiversity and habitats, land degradation, and deterioration of air quality [11]. Evidence shows that haphazard disposal of tannery wastewater into the environment has left the quality of the Modjo River in Ethiopia [8], the Buriganga River in Bangladesh [6]. and the groundwater quality of Kasur City in Pakistan [12], and that in Kano City in Nigeria [7] in grievous states. Satisfactory treatment of this wastewater is mandatory to attain public and environmental health and also to meet Sustainable Development Goal 6, specifically Target 6.3, which aims at reducing the fraction of untreated wastewater by 2030 [13].

Over the years, various treatment technologies have been developed for tannery wastewater, comprising biological treatment, micro- and ultrafiltration, coagulation and flocculation, electrocoagulation, ozonation, adsorption, and reverse osmosis [14]. Most of these treatment processes, specifically ozonation, reverse osmosis, electrocoagulation, micro- and ultrafiltration, despite their efficacy, have some major limitations, such as sophisticated treatment processes and operation, large installation and operation costs as well as high energy requirements [15, 16]. Coagulation–flocculation process is mostly suitable for the removal of colloidal substances from wastewater [17, 18]. Its major limitation lies in its large sludge production and ineffective removal of certain contaminants, such as colour and soluble COD, from wastewater [16, 19]. Biological treatment, which is considered an economical treatment process, is also inefficient in treating tannery wastewater due to the occurrence of some toxic and recalcitrant organic compounds, such as tannins employed in transforming animal skins into leather [20]. In comparison to these technologies, adsorption, a physicochemical treatment process that involves the removal of contaminants from wastewater through the attachment of these pollutants onto solid surfaces [21], has been widely adopted for the treatment of wastewater due to its insensitivity to wastewater toxicity, low sophistication, easy operability and ultimately its efficiency in removal of pollutants [22], including colour and recalcitrant COD from wastewater [23].

The primary adsorbent applied in the adsorptive treatment of wastewater has been conventional activated carbon. It has proven to be very efficacious in taking out various pollutants from wastewater [24]. The major drawback of this adsorbent is related to its costliness and the pitfalls regarding its regeneration [24]. This has necessitated the need for the search and development of alternative adsorbents, which are not only effective but also less expensive. Different adsorbents have been developed from waste materials, such as rice husks [19], fly ash [25], tea leaves [26], shrimp shells [27], teff husks [28], moringa seeds [29], bone char [30], neem leaves, and tamarind tree bark [31], for removal of contaminants such as chromium, colour, turbidity, and biochemical oxygen demand from tannery wastewater. Among these adsorbents, bone char manufactured from animal bones, a common waste product from slaughterhouses, which has proven to be a very promising adsorbent in the removal of fluorides [32], heavy metals [33, 34], and methylene blue [35] from various kinds of aqueous media will be used in this study for the adsorption of COD and colour from tannery wastewater.

From the literature, batch-mode configuration experiments are commonly applied in determining the adsorption capacities of adsorbents, the effect of process parameters, and the mechanisms involved in adsorption processes [36]. However, data obtained from such experiments are only suitable for low wastewater flow rates and are not practically beneficial in industries generating high wastewater flows [37]. Fixed bed adsorption configurations operating under continuous flow conditions are more preferable due to their efficiency, ease of operation [23], and their ability to provide relevant data for the design and scale-up of adsorption columns for industrial applications [38]. From an in-depth literature search conducted, no study has reported on dynamic modelling on the utilisation of bone char for the elimination of COD and colour from tannery wastewater using fixed bed adsorption columns. Alam et al. [30] assessed the applicability of activated bone charcoal for the treatment of chrome tannery wastewater in removing suspended solids, biochemical oxygen demand, dissolved solids, and COD through column studies but did not delve into the implications of different process conditions and the dynamic modelling of adsorption in the fixed bed column.

To close this knowledge gap, this study sought to evaluate the performance of bone char, the effect of operating parameters, and the fitting of suitable models to the adsorption of COD and colour from tannery wastewater in a fixed bed column. The influence of relevant design parameters, such as bed height and flow rate, on the adsorption process was assessed, and the resulting breakthrough curves were modelled using the Thomas, Adams–Bohart, and Yoon–Nelson dynamic models.

2. Research Methodology

2.1. Sampling and Characterisation of Wastewater. Samples of tannery wastewater were taken from the Aboabo Tannery in Ghana. Prior to the adsorption studies, the wastewater was treated with aluminium sulphate and cassava starch through a coagulation–flocculation process to remove the colloidal substances. Performance of the laboratory analyses on the samples were carried out in accordance with the Standard Methods for Examination of Water and Wastewater [39]. The turbidity and pH of the wastewater were determined using a HANNA turbidimeter (HI 93414) and a Milwaukee MW 101 pH meter, respectively. In analysing the COD and colour of the wastewater, the HACH methods, accompanied with the HACH DR 3900 spectrophotometer, were employed. Sample dilution techniques coupled with dissolved oxygen measurements were applied in evaluating the 5-day biochemical oxygen demand (BOD_5) of the wastewater samples.

2.2. Preparation of Bone Char. The bone char employed as an adsorbent in this research work was produced from dried head bones of cattle collected from the Kumasi Abattoir in Ghana. The raw bones were crushed into smaller sizes. They were then washed well using tap water initially and finally distilled water to remove any dirt. The bones were oven-dried overnight at 110°C and then pyrolysed in a muffle

furnace at 700°C for 2 hr at a heating rate of 13.33°C/min [40]. The bone char was crushed and sieved. Particle sizes ranging from 0.15 to 0.5 mm were used in the fixed-bed column experiments.

2.3. Bone Char Characterisation. The manufactured bone char was characterised by applying the following analytical methods: Fourier transform infrared (FTIR) spectrometer, scanning electron microscope (SEM) with energy-dispersive X-ray spectrometry (EDS) detector, and Brunauer–Emmett–Teller (BET) surface area. An FTIR spectrometer (IRTracer 100) was applied to investigate the functional groups on the surface of the bone char within a range of 4,000 and 350 cm^{-1} wavelength. Evaluation of the chemical composition and the surface morphology of the bone char was performed with the aid of the SEM (JEOL JSM-6060S) and an EDS detector (GATR10). Information on the specific surface area of the char was attained by employing the BET procedure, while the prediction of the size and distribution of the pores was determined using the Barrett–Joyner–Halenda (BJH) method. The resulting data on the surface area and the pore size distribution were analysed with the help of the BEL Master software through adsorption–desorption isotherms. The characteristic micro- or mesoporous nature of the char was detected with a Nitrogen adsorption apparatus—BELSorp-Mini II-SKV (Microtrac Retsch Ltd.). Other characteristics of the bone char regarding the yield, bulk density, pH, and point of zero charges are explicitly explained in a previous research work [9] conducted by the authors of this study in which the efficacy of bone char as an adsorbent, as well as the adsorption mechanisms involved in COD and colour removal from tannery wastewater through adsorption batch experiments, were investigated.

2.4. Adsorption Column Experiments. To evaluate the dynamic behaviour of COD and colour adsorption onto bone char, fixed bed columns with internal diameters of 2.7 cm and lengths of 25 cm were employed. The columns were operated under gravity. The height of the column beds was varied at three [3] different lengths (5, 10, and 15 cm), which was equivalent to 16.42, 32.01, and 48.11 g of bone char, respectively. A stainless-steel mesh was fixed at the base of each column. The columns were loaded with a glass wool of 2 cm height at the bottom, followed by the bone char, cotton wool, and then gravels. The glass wool was used to prevent loss of the bone char as well as to ensure tightly packed column beds. Control valves were used to regulate the flow of the influent into the columns and the exit of the treated wastewater. Distilled water was passed through the columns to allow trapped air to escape. A diagram of the experimental setup for the adsorption column is illustrated in Figure 1.

A series of experiments were performed to determine the effect of different wastewater flow rates (2, 5, and 8 mL/min) and bed heights (5, 10, and 15 cm) on the adsorption of COD and colour onto the bone char. All experiments were performed at room temperature. Treated wastewater samples were fetched at specific time periods for COD and colour analyses. Triplicate experiments were conducted. The average of the results obtained was computed and used in the analysis.

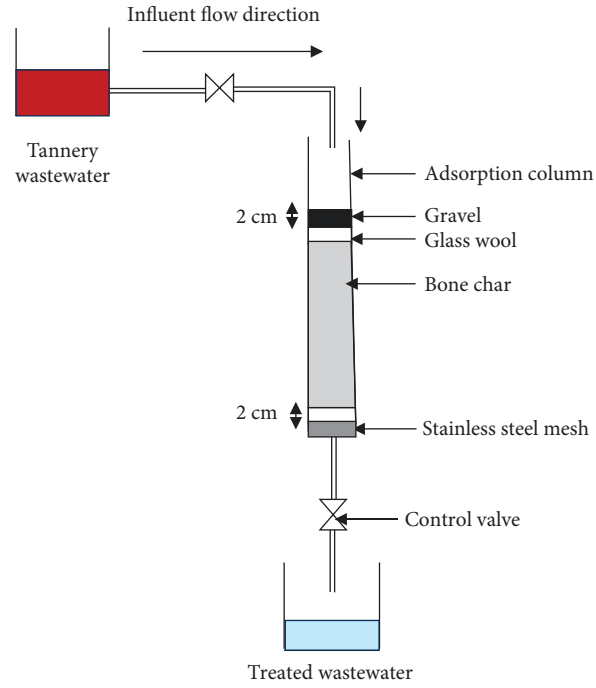

FIGURE 1: Experimental set-up for fixed bed adsorption column packed with bone char.

2.5. Development of Breakthrough Curves. In assessing the efficacy of the fixed bed adsorption columns for the removal of COD and colour from the tannery wastewater, data obtained from the column experiments were analysed using breakthrough curves. The breakthrough curves described the adsorption of COD and colour onto the bone char in a fixed bed column [41]. Process conditions, including wastewater flow rate and bed height, influence the characteristic shape of the breakthrough curve and the performance of the adsorption column [42].

A plot of the quotient, C_t/C_o (that is a division of the effluent concentration (C_t) by the influent concentration (C_o)), against service time (t) generates the breakthrough curve. The point of exhaustion in the columns was considered to occur at a service time, t_e when C_t was 99.5% of the influent concentration [42]. From the breakthrough curves, design parameters namely; adsorption capacity of the column (q_{total}), total volume of treated wastewater (V_{eff}), total amount of COD or colour adsorbed (m_{total}), total percentage of COD or colour removed (R) and the equilibrium adsorption capacity, q_e were computed according to Equations (1)–(5) [41, 42].

The adsorption capacity of the column (q_{total}) for removal of COD (mg/g) and colour (Pt-Co/g) were evaluated according to Equation (1).

$$q_{total} = \frac{Q}{1{,}000}(C_o - C_t)t_{total}, \quad (1)$$

where C_o and C_t represent the initial and adsorbed concentration of COD (mg/L) or colour (Pt-Co/L), Q is the flow rate (mL/min) and t_{total} is the total flow time (min).

The total volume of treated wastewater (effluent), V_{eff} in mL was evaluated according to Equation (2).

$$V_{\text{eff}} = Qt_{\text{total}}. \quad (2)$$

The total amount of COD (mg) or colour (Pt-Co) adsorbed, m_{total} that passed through the column is also given, as shown in Equation (3).

$$m_{\text{total}} = \frac{C_{\text{o}} \times Q \times t_{\text{e}}}{1{,}000}. \quad (3)$$

The total percentage of COD or colour removed, R (%), was calculated according to Equation (4).

$$R(\%) = \frac{q_{\text{total}}}{m_{\text{total}}} \times 100. \quad (4)$$

The equilibrium adsorption capacity, q_e for COD (mg/g) or colour (Pt-Co/g), was calculated based on Equation (5).

$$q_{\text{e}} = \frac{q_{\text{total}}}{m}, \quad (5)$$

where m denotes the mass of the bone char used (g).

2.6. Dynamic Models. The design of adsorption columns requires the application of models to breakthrough curves to obtain design parameters. Among them, the Thomas, Adams–Bohart, and Yoon–Nelson models were adopted in this study.

2.6.1. Thomas Model. The Thomas dynamic model is widely applied in the description of the adsorption performance of fixed bed columns and the prediction of breakthrough curves. The model assumes that the driving force of the reaction rate follows the reversible second-order reaction kinetics [42]. The model in its linearised form is expressed, as shown in Equation (6).

$$\text{Ln}\left(\frac{C_{\text{o}}}{C_{\text{t}}} - 1\right) = \frac{K_{\text{TH}} q_{\text{o}} m}{Q} - K_{\text{TH}} C_{\text{o}} t, \quad (6)$$

where K_{TH} is the Thomas rate constant (mL/(min mg) for COD) or (mL/(min Pt-Co) for colour), q_{o} is the equilibrium adsorption capacity ((mg/g) for COD) or ((Pt-Co/g) for colour), m is the mass of the adsorbent used (g), C_{o} is the initial COD (mg/L) or colour (Pt-Co/L) concentration, C_{t} is the effluent COD (mg/L) or colour (Pt-Co/L) concentration at a particular flow time, t (min) and Q is the flow rate (mL/min). The values of K_{TH} and q_{o} were obtained from the intercept and the slope of the plot of $\ln[(C_{\text{o}}/C_{\text{t}}) - 1]$ against time, t.

2.6.2. Adams–Bohart Model. The Adams–Bohart model assumes that the adsorption rate primarily depends on the original concentration of the pollutants and the remaining adsorption capacity of the adsorbent material. It gives a description for only the first portion of the breakthrough curve [23]. The linear equation of the Adams–Bohart model is written, as shown in Equation (7) [43].

$$\text{Ln}\frac{C_{\text{t}}}{C_{\text{o}}} = k_{\text{AB}} C_{\text{o}} t - k_{\text{AB}} N_{\text{o}} \frac{z}{k_{\text{AB}} U_{\text{o}}}, \quad (7)$$

where k_{AB} is the Adams–Bohart rate constant ((L/(min mg) for COD) or ((L/(min Pt-Co) for colour), z is the bed depth (cm), N_{o} is the saturation concentration ((mg/L) for COD) or ((Pt-Co/L) for colour) and U_{o} is the linear velocity of the influent. U_{o} is computed by dividing the volumetric flow rate by the area of the column. The constants k_{AB} and N_{o} were obtained from the slope and the intercept of the linear plot of $\ln\frac{C_{\text{t}}}{C_{\text{o}}}$ against t.

2.6.3. Yoon–Nelson Model. The Yoon–Nelson model assumes that the rate in the probability of adsorbate adsorption declines based on the probability of adsorbate adsorption as well as the probability of the breakthrough of the adsorbate on the adsorbent material [23]. It is a less complicated model as it does not rely on data regarding the adsorbent type, properties of the fixed bed adsorption column, and nature of adsorbate molecules. The linear equations of the Yoon–Nelson model are expressed as Equation (8) [43].

$$\text{Ln}\frac{C_{\text{t}}}{C_{\text{o}} - C_{\text{t}}} = k_{\text{YN}} t - \tau k_{\text{YN}}, \quad (8)$$

where k_{YN} is the Yoon–Nelson rate constant (1/min) and τ is the time required to achieve a 50% adsorbate breakthrough. The values of the constants k_{YN} and τ were computed from the slope and intercept of a linear plot of $\ln\frac{C_{\text{t}}}{C_{\text{o}} - C_{\text{t}}}$ against time, t.

Table 1: Characteristics of vegetable tannery wastewater.

Parameter	Value	Ghana EPA standard [44]
pH	3.15 ± 0.11	6.0–9.0
Colour (Pt-Co)	$4{,}050 \pm 128$	100
Turbidity (NTU)	180.64 ± 54	75
COD (mg/L)	$15{,}800 \pm 120$	250
BOD_5 (mg/L)	675.35 ± 65	50

3. Results and Discussion

3.1. Tannery Wastewater Characteristics. The characteristics of the vegetable tannery wastewater are displayed in Table 1. The wastewater has a low pH depicting its acidic nature. It is also strongly coloured with high levels of turbidity and organic matter. None of the parameters fell within the standard guidelines for wastewater discharge set by the Ghana Environmental Protection Agency [44]. More specifically, the concentrations of colour and COD were 40% and 63% above the stipulated threshold limits, respectively.

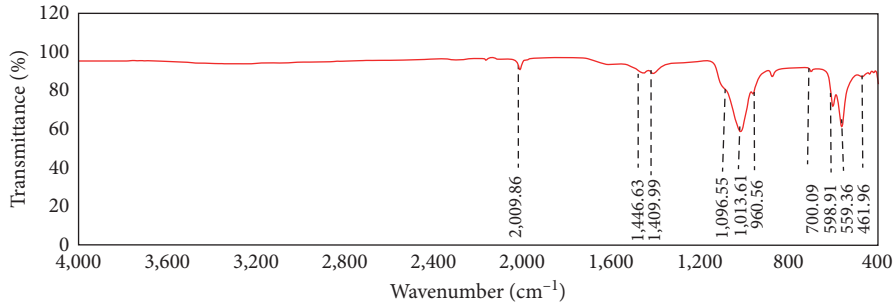

Figure 2: FTIR spectra of bone char.

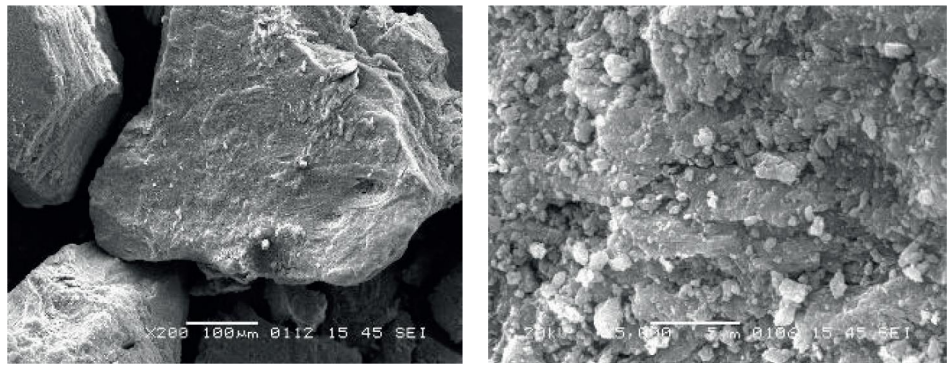

(a) (b)

Figure 3: SEM images of bone char at (a) 200x and (b) 5,000x magnifications.

3.2. Characteristics of the Bone Char

3.2.1. Surface Functional Groups of the Bone Char. The various surface functional groups on the bone char are displayed in the FTIR spectra shown in Figure 2. The band width within the 2,029 and 1,979 cm^{-1} wavelength peaking at 2,009.86 cm^{-1} depicts the presence of phosphate ions (PO_4^{3-}). Within the bandwidth regions of 1,500 and 1,390 cm^{-1} with a double peak occurring at 1,446 and 1,410 cm^{-1} represents the functional groups of collagen and other proteinaceous substances on the char, namely, carbonate (CO_3^{2-}), carboxylate ($-COO^-$) and ammonium (NH_4^+) ions as well as alkene and alkyl functional groups with a C–H bend overlap. Functional groups of amines with a C—N stretch and that of phosphate with a P—O asymmetric stretching are displayed within the bandwidth of 1,090 and 1,020 cm^{-1}. The peak at 870 cm^{-1} wavelength is attributed to a carbonate ion. The bands within 960, 600, 559, and 462 cm^{-1} correspond to phosphate functional groups. Other functional groups, including O—H bend and C—Cl stretch, occurred within 700 and 650 cm^{-1} bandwidths. The peaks within the 610 and 550 cm^{-1} range could be linked to the existence of calcium ions (Ca^{2+}) [45]. The FTIR spectra of the head bone char of cattle shown in this study agree with the results documented by Rojas-Mayorga et al. [46].

3.2.2. Surface Area and Pore Size of Bone Char. From the BET analysis, the specific surface area of the bone char was 129.22 m^2/g. The total pore volume and average pore size of the char were 0.3424 cm^3/g and 10.88 nm, respectively. The pore size falling within the range of 2–50 nm of the IUPAC classification is a clear indication of the mesoporous nature of the bone char. Escape of the volatile compounds during pyrolysis of the raw cattle bones led to the formation of the mesopores within the inorganic components of the bones, specifically the calcium carbonate and hydroxyapatite. Similar results on the surface characteristics of the bone char were obtained by Saffari and Moazallahi [33], who investigated the adsorption of nickel onto bone char.

3.2.3. Surface Morphology of Bone Char. The images of the morphology of the bone char attained from scanning electron micrographs at different magnifications are illustrated in Figures 3(a) and 3(b). The images reveal the irregularity in the shape of the particles of the bone char and their rough surfaces. The rough surfaces, which signify the pores on the surface of the bone char, play an essential role in the adsorption of contaminants from wastewater. Similar surface morphological images were presented by Shahid et al. [47].

3.2.4. Elemental Composition of Bone Char. The spectrum and quantitative data obtained from the EDS analysis on the bone char are shown, respectively, in Figure 4 and Table 2. The quantitative data presents the major elemental composition of the bone char as oxygen, calcium, phosphorus, and carbon. The larger proportions of calcium and phosphorus ions in the bone char confirm the presence of the hydroxyapatite salt ($Ca_{10}(PO_4)(OH)_2$), the principal inorganic component of bone char, which plays a critical role in the removal of most contaminants from polluted water. The molar ratio of calcium to phosphorus (Ca/P) was

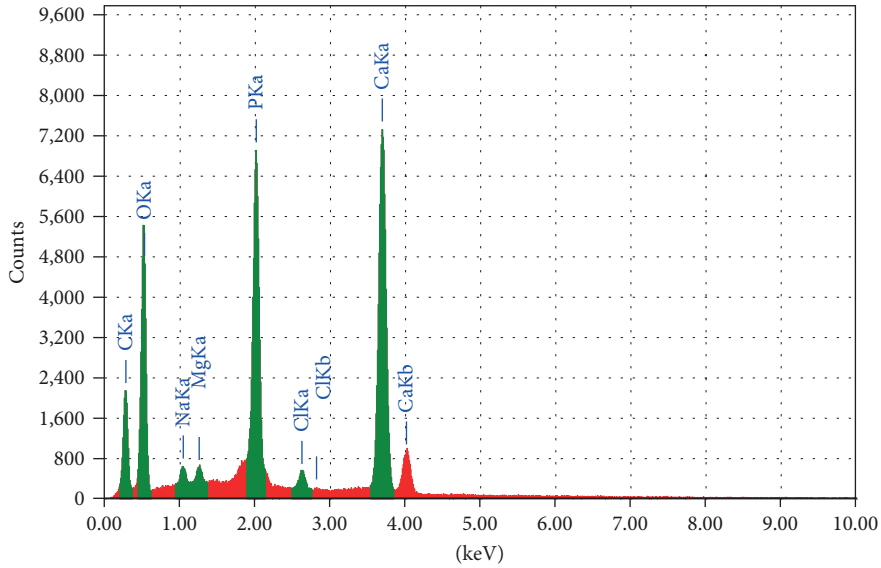

Figure 4: EDS spectrum of bone char.

Table 2: EDS quantitative data on bone char.

Element	Weight (%)	Atomic (%)
O	39.19	50.01
C	13.70	23.29
Ca	30.46	15.52
P	14.11	9.30
Na	0.82	0.73
Cl	1.08	0.62
Mg	0.64	0.53
Total	100	100

precisely 1.67. This value matches exactly with the stoichiometric value of a pure hydroxyapatite [48]. Other ions, including sodium (Na), magnesium (Mg), and chlorides (Cl^-), occur in minor concentrations in the bone char. These results affirm the similar observations made by Shahid et al. [47].

3.3. Performance of Adsorption Column at Different Operating Conditions

3.3.1. Effect of Wastewater Flow Rate. The effect of volumetric flow rate on the adsorption of COD and colour onto bone char was assessed by varying the flow rate at 2, 5, and 8 mL/min while keeping the bed height constant at 10 cm. The COD and colour concentrations of the influent averaged 15,800 mg/L and 4,050 Pt-Co/L, respectively. The breakthrough curves for adsorption of COD and colour are illustrated in Figures 5(a) and 5(b). The corresponding design parameters are presented in Tables 3 and 4 for adsorption of COD and colour, respectively. Observation of Figures 5(a) and 5(b) show that as the flow rates increased the breakthrough curves became steeper, the time at which saturation occurred became shorter, and the removal efficiency of COD and colour also declined. Hence, from Table 3, an increase in flow rate from 2 to 8 mL/min resulted in a reduction in the saturation time from 325 to 120 min with a corresponding decline in the COD removal efficiency from 74.60% to 61.54%. Similarly, for the adsorption of colour, an increase in flow rate from 2 to 8 mL/min led to a decrease in the saturation time from 210 to 90 min with a corresponding drop in the removal efficiency from 82.35% to 66.67% (Table 4). At higher flow rates, there is a decline in the mass transfer resistance due to the high velocity in the movement of the adsorption zone through the column, resulting in a shorter residence time of the contaminants in the column. This explains the shorter saturation time and the steep breakthrough curves that were observed at higher flow rates. Furthermore, high flow rates resulted in a short residence time of the contaminants in the column and, hence, an insufficient time for the molecules of the contaminants to diffuse into the bone char, leading to lower adsorption efficiencies. On the other hand, as the contaminants had longer contact time with the bone char at lower flow rates, higher adsorption efficiencies and longer saturation times were attained. Such an observation was also made by Yahuza et al. [49]. As the highest adsorption efficiencies of COD and colour from the wastewater were observed at the lowest flow rate of 2 mL/min, this value was selected as the optimum flow rate.

3.3.2. Effect of Bed Height. The effect of bed height on the breakthrough curves was studied at different bed heights of 5, 10, and 15 cm at a fixed flow rate of 2 mL/min. The influent COD and colour concentrations of the wastewater were 15,800 mg/L and 4,050 Pt-Co/L, respectively. The breakthrough curves indicating the performance of the adsorption columns at the various bed heights are shown in Figures 6(a) and 6(b). The design parameters for the fixed bed columns are also presented in Table 5 for COD and Table 6 for colour.

From the Tables 5 and 6, a rise in the bed height yielded a corresponding increase in the breakthrough time, volume of treated wastewater, and adsorption efficiencies. The bed height of the adsorption column is linked to the mass of

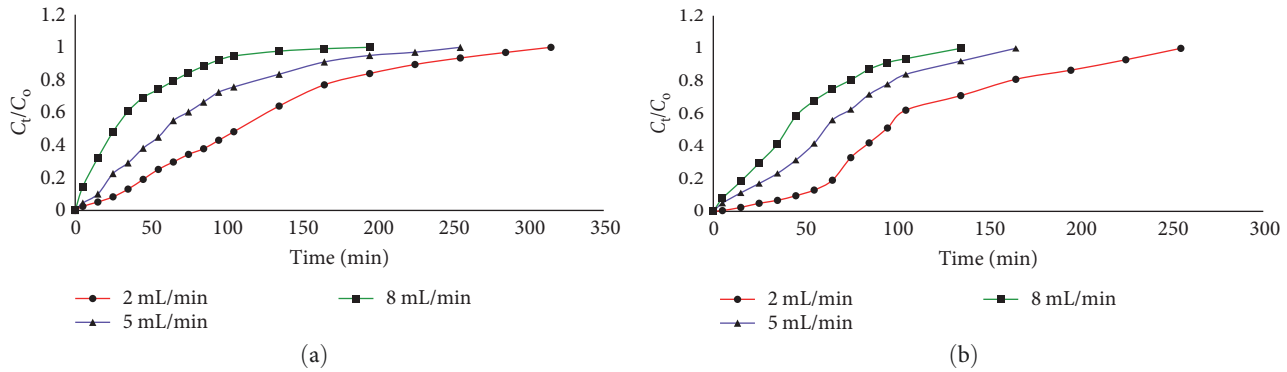

Figure 5: Breakthrough curves for (a) COD and (b) colour adsorption onto bone char at different flow rates (initial COD concentration of 15,800 mg/L, initial colour concentration of 4,050 Pt-Co/L, bed height of 10 cm).

Table 3: Fixed bed column design parameters for adsorption of COD onto bone char at different flow rates.

Q (mL/min)	t_{total} (min)	V_{eff} (mL)	m_{total} (mg)	q_{total} (mg)	q_e (mg/g)	Removal (%)
2	235	470	9,954	7,426	231.99	74.60
5	160	800	17,775	12,640	394.88	71.11
8	120	960	24,648	15,168	473.85	61.54

Table 4: Fixed bed column design parameters for adsorption of colour onto bone char at different flow rates.

Q (mL/min)	t_{total} (min)	V_{eff} (mL)	m_{total} (Pt-Co)	q_{total} (Pt-Co)	q_e (Pt-Co/g)	Removal (%)
2	210	420	2,066	1,701	53.14	82.35
5	127	635	3,341	2,572	80.36	76.98
8	90	720	4,374	2,916	91.10	66.67

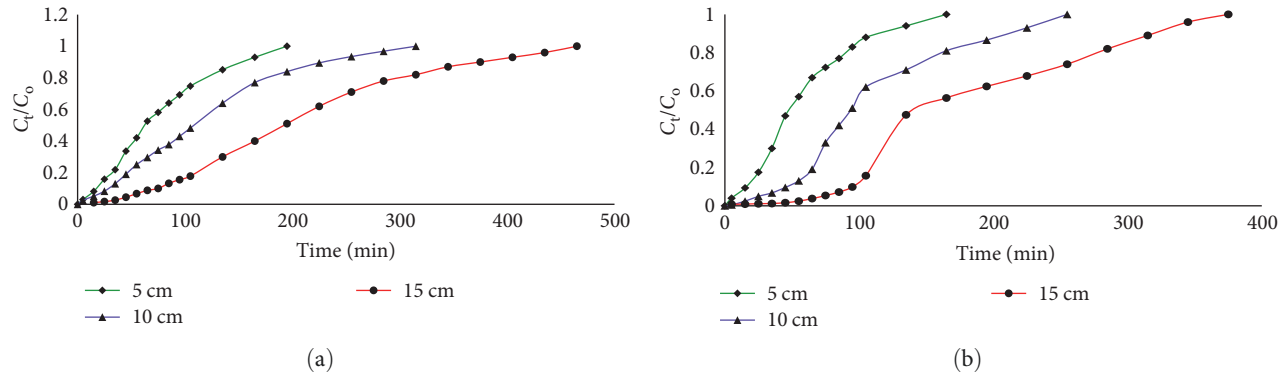

Figure 6: Breakthrough curves for (a) COD and (b) colour adsorption onto bone char at different bed heights (initial COD concentration of 15,800 mg/L, initial colour concentration of 4,050 Pt-Co/L, flow rate of 2 mL/min).

the bone char used, which represents the free adsorption sites [50]. Therefore, an increase in bed height resulted in a higher adsorption efficiency due to the increased number of adsorption sites. Additionally, an increase in bed height prolonged the contact time between the contaminants and the bone char, which allowed sufficient time for diffusion of the contaminants into the bone char to occur [42]. As a result, longer saturation times, higher volumes of treated wastewater, and enhanced adsorption efficiencies were noted at higher bed heights. Accordingly, the adsorption efficiency increased from 73.85% to 80.65% for COD (Table 5) and from 66.85% to 84% for colour (Table 6), with an increase in bed height from 5 to 15 cm. The slopes of the breakthrough curves being steeper at lower bed heights can be attributed to the short residence time of the pollutants in the adsorption column (Figures 6(a) and 6(b)). These results suggest that higher bed heights are most appropriate for COD and colour adsorption in the fixed bed columns.

Table 5: Design parameters for fixed bed adsorption of COD onto bone char at varying bed heights.

H_T (cm)	t_{total} (min)	V_{eff} (mL)	m_{total} (mg)	q_{total} (mg)	q_e (mg/g)	Removal (%)
5	144	288	6,162	4,550.40	277.13	73.85
10	235	470	9,954	7,426	231.99	74.60
15	375	750	14,694	11,850	227.40	80.65

Table 6: Design parameters for fixed bed adsorption of colour onto bone char at varying bed heights.

H_T (cm)	t_{total} (min)	V_{eff} (mL)	m_{total} (Pt-Co)	q_{total} (Pt-Co)	q_e (Pt-Co/g)	Removal (%)
5	110	221	1,336.50	893.43	54.41	66.85
10	210	420	2,065.50	1,701.00	53.14	82.35
15	315	630	3,037.50	2,551.50	53.03	84.00

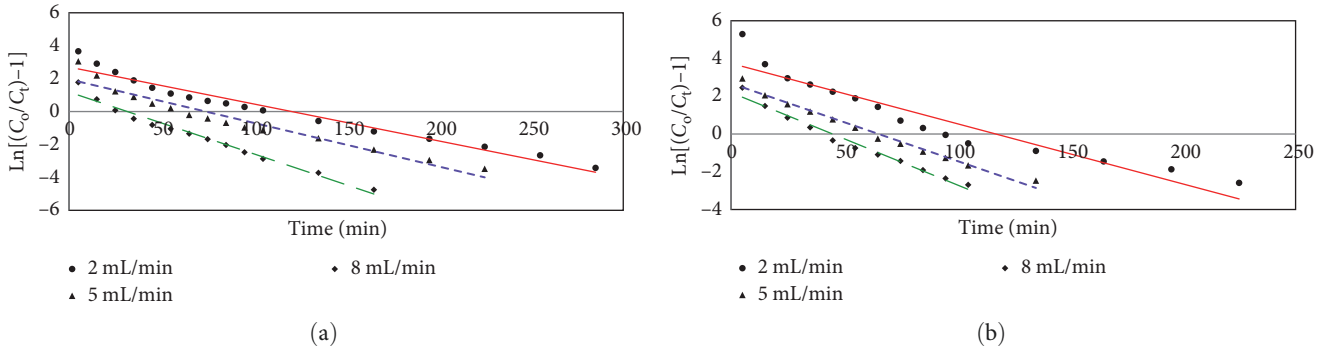

Figure 7: Linear plots of the Thomas model showing the effect of flow rate on adsorption of (a) COD and (b) colour onto bone char (inlet concentration of COD of 15,800 mg/L, inlet concentration of colour of 4,050 Pt-Co/L, bed height of 10 cm).

3.4. Application of Adsorption Column Models. The experimental data from the fixed bed column studies were fitted to the Thomas, Adam–Bohart, and Yoon–Nelson models.

3.4.1. Application of the Thomas Model. The Thomas model was adopted to predict the maximum adsorption capacity (q_o) and the adsorption rate constant (K_{TH}). The linear plots of $\ln[(C_o/C_t) - 1]$ and time for both adsorption of COD and colour are shown in Figures 7(a), 7(b), 8(a), and 8(b), respectively. The values obtained for q_o and K_{TH} for both COD and colour removal at different flow rates and bed heights are presented in Table 7. An increase in flow rate from 2 to 8 mL/min enhanced the adsorption rate constant and adsorption capacities for both COD and colour removal (Table 7). However, increasing the bed height from 5 to 15 cm resulted in a decline in the adsorption rate constant but an increase in the adsorption capacities for both COD and colour (Table 7). The enhancement of the adsorption capacity at high bed depth can be explained by the augmented number of free sites available for adsorption. A similar trend was obtained by Vishali et al. [50]. The predicted adsorption capacities of the Thomas model (Table 7) were lower than the experimental values (Tables 5 and 6), connoting that the Thomas model could not adequately elucidate the adsorption system, even though high regression correlation coefficient (R^2) values ranging from 0.9037 and 0.9796 were obtained. Conclusively, the Thomas model is not a suitable model for the design of the adsorption columns. Similar observations were reported by Acheampong et al. [51]. The failure of the Thomas model to sufficiently describe the breakthrough data shows that the adsorption process involved in the adsorption of COD and colour onto bone char does not follow the Langmuir isotherm as is assumed by the model [52]. This observation confirms the results from an earlier research conducted by the authors of this study which indicated that the adsorption process involved in COD and colour adsorption from tannery wastewater onto bone char follows the Freundlich isotherm [9]. Additionally, the poor fit of the Thomas model to the experimental results refutes another underlying assumption of the model, which states that resistances resulting from internal and external diffusion do not govern the rate-limiting step of a reaction [53].

3.4.2. Adams–Bohart Model. The values of the constants, namely, the Adams–Bohart rate constant (K_{AB}) and the saturation concentration (N_o)of the Adams–Bohart model presented in Table 8 for COD and colour adsorption were computed from the linear plots shown in Figures 9(a), 9(b), 10(a), and 10(b) for varying flow rates and bed heights, respectively. The values of K_{AB} for COD removal lowered at increased flow rates and bed heights, as was reported by Lopez–Cervantes et al. [53]. For colour removal, the values of K_{AB} increased marginally at heightening flow rates but declined with an increase in bed height. The values of N_o, on the other hand, rose with increasing flow rate but dropped

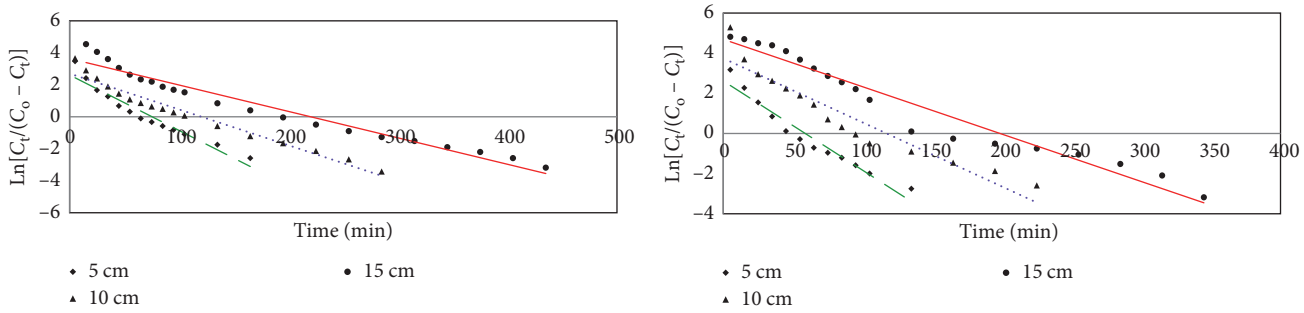

Figure 8: Linear plots of the Thomas model showing the effect of bed height on adsorption of (a) COD and (b) colour onto bone char (inlet concentration of COD of 15,800 mg/L, inlet concentration of colour of 4,050 Pt-Co/L, flow rate of 2 mL/min).

Table 7: Thomas model parameters for fixed bed adsorption of COD and colour under varying flow rates and bed heights.

Q (mL/min)	H (cm)	COD			Colour		
		K_{TH} (L/(min mg) x10^{-6})	q_o (mg/g)	R^2	K_{TH} (L/(min Pt-Co) x10^{-5})	q_o (Pt-Co/g)	R^2
2	10	1.42	119.05	0.9586	0.78	29.69	0.9037
5	10	1.68	182.23	0.9303	1.01	41.36	0.9830
8	10	2.37	124.749	0.9743	1.21	45.46	0.9796
2	5	2.20	144.94	0.9586	1.11	28.99	0.9468
2	15	1.04	144.86	0.9339	0.58	33.46	0.9537

Table 8: Adams–Bohart model parameters for fixed bed column adsorption of COD and colour onto bone char under different flow rates and bed heights.

Q (mL/min)	H (cm)	COD			Colour		
		K_{AB} (L/(min mg) x10^{-7})	N_o (mg/L)	R^2	K_{AB} (L/(min Pt-Co) x10^{-6})	N_o (Pt-Co/L)	R^2
2	10	5.95	34,518.57	0.7091	4.12	7,037.56	0.6889
5	10	5.63	66,427.78	0.5875	4.25	11,483.21	0.78
8	10	4.49	77,725.48	0.5388	4.25	14,816.32	0.7356
2	5	9.43	41,710.46	0.6761	4.32	8,741.69	0.6748
2	15	5.51	34,641.13	0.7811	3.51	7,191.30	0.8291

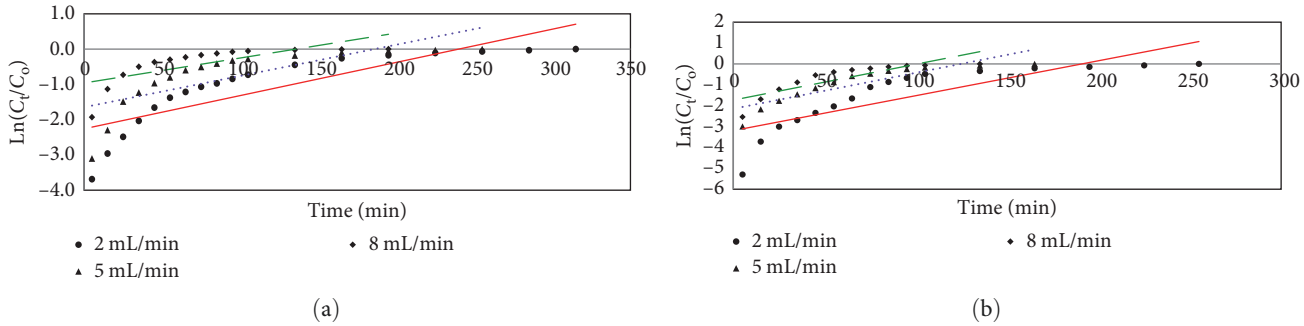

Figure 9: Linear plots of the Adams–Bohart model showing the effect of flow rate on adsorption of (a) COD and (b) colour onto bone char (inlet concentration of COD of 15,800 mg/L, inlet concentration of colour of 4,050 Pt-Co/L, bed height of 10 cm).

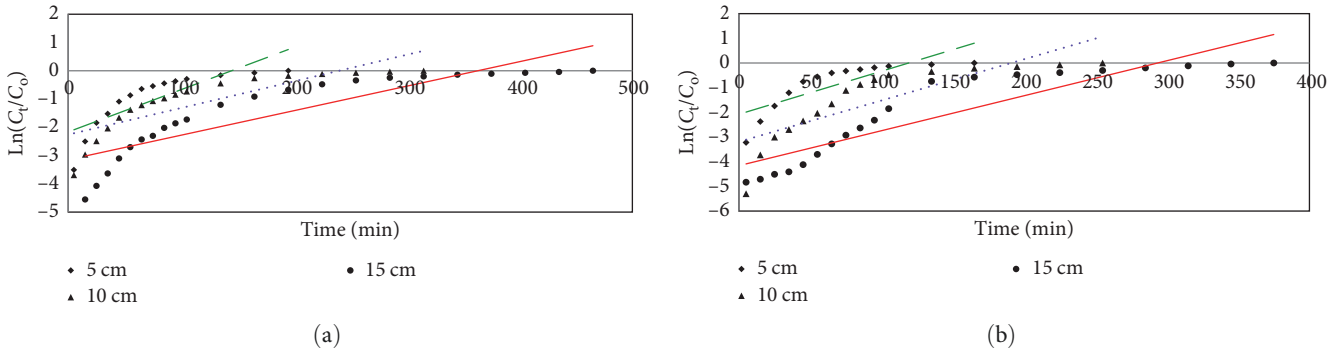

Figure 10: Linear plot of Adams–Bohart model showing the effect of bed height on adsorption of (a) COD and (b) colour onto bone char (inlet concentration of COD of 15,800 mg/L, inlet concentration of colour of 4,050 Pt-Co/L, flow rate of 2 mL/min).

Table 9: Yoon–Nelson model parameters for fixed bed adsorption of COD and colour under different flow rates and bed heights.

Q (mL/min)	H (cm)	COD				Colour			
		K_{YN} (1/(min) x10^{-2})	τ (min)	τ, exp (min)	R^2	K_{YN} (1/(min) x 10^{-2})	τ (min)	τ, exp (min)	R^2
2	10	2.24	120.59	110.00	0.9587	3.19	117.34	95.00	0.9037
5	10	2.65	73.85	60.00	0.9303	4.10	65.38	60.82	0.9830
8	10	3.75	31.59	45.00	0.9743	4.89	44.92	40.00	0.9796
2	5	3.47	75.31	62.54	0.9339	4.45	58.76	50.50	0.9468
2	15	1.65	220.55	194.00	0.9580	2.36	198.75	140.0	0.9537

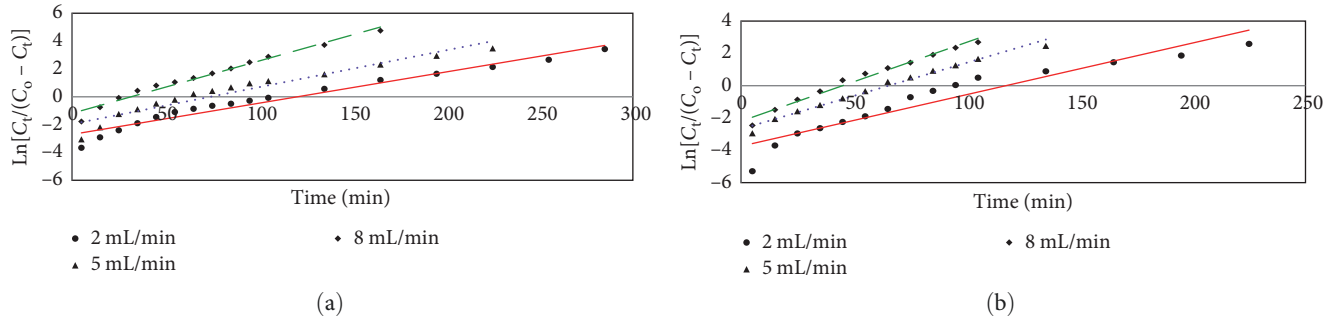

Figure 11: Linear plots of the Yoon–Nelson model showing the effect of flow rate on adsorption of (a) COD and (b) colour onto bone char (inlet concentration of COD of 15,800 mg/L, inlet concentration of colour of 4,050Pt-Co/L, bed height of 10 cm).

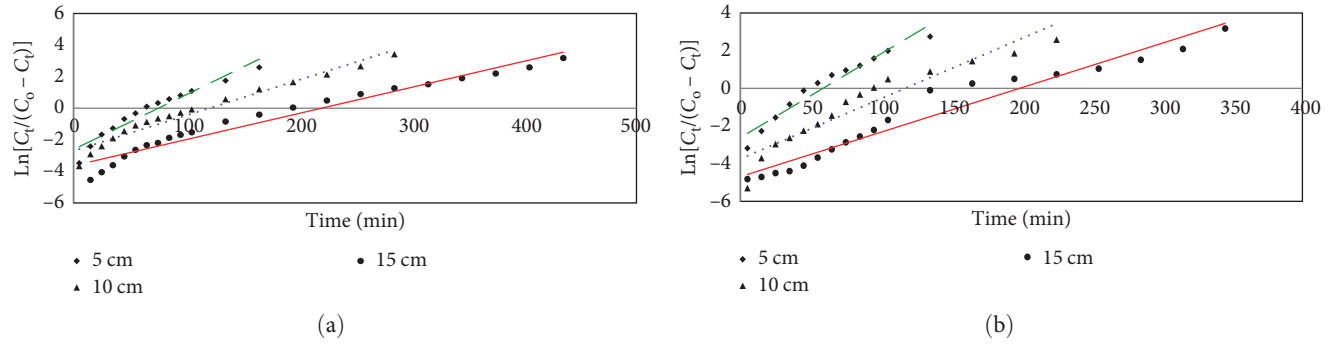

Figure 12: Linear plots of the Yoon–Nelson model showing the effect of bed height on adsorption of (a) COD and (b) colour onto bone char (inlet concentration of COD of 15,800 mg/L, inlet concentration of colour of 4,050 Pt-Co/L, flow rate of 2 mL/min).

Table 10: Comparison of the performance of different adsorbents in the removal of colour and COD from wastewater.

Adsorbent	Type of wastewater	Initial concentration (mg/L)	Bed height (cm)	Flow rate (mL/min)	Maximum adsorption capacity	Adsorption efficiency (%)	Reference
Adsorption of COD							
Magnetite–zeolite A composite	Textile	30	5	4	101.66 mg/g	—	[55]
Rattan-activated carbon	Cotton textile mill	—	8	10	73.23 mg/g	—	[56]
Palm kernel-activated carbon	Domestic greywater	421	20	5	56.60 mg/g	—	[57]
Zeolite and granular activated carbon	Dye	—	20	—	—	59.46	[58]
Shale	Textile	5,600	30	—	—	97.31	[59]
Bone char	Tannery	15,800	15	2	227.40 mg/g	80.65	Present study
Adsorption of colour							
Zeolite and granular activated carbon	Dye	—	20	—	—	58.40	[58]
Shale	Textile	2,105	30	—	—	98.20	[59]
Bone char	Tannery	4,050	15	2	53.03 Pt-Co/g	84.00	Present study

with increased bed height for both COD and colour removal. An equivalent trend in the results was reported by Vishali et al. [50]. The low R^2 values ranging from 0.5388 to 0.8291 depict that the Adams–Bohart model is not a good predictor of the breakthrough curves for adsorption of COD and colour from the tannery wastewater onto the bone char.

The Adams–Bohart model presumes that the rate of adsorption of a species is proportionally dependent on the residual adsorption capacity of an adsorbent, and the concentration of the sorbing species is a symmetrical sigmoidal function [54]. Hence, the inability of the model to adequately fit the experimental data portrays that the breakthrough curves are asymmetric. This asymmetry may be due to the involvement of intraparticle diffusion, which plays a dominant role in the mechanism of adsorption as the rate-determining step of the adsorption process [9, 54].

3.4.3. Yoon–Nelson Model. The results of the Yoon–Nelson constants, τ and K_{YN} representing the time period to obtain 50% breakthrough and the rate constant, respectively, are displayed in Table 9. Surges in flow rates caused increases in K_{YN} values but drops in τ values for both COD and colour removal. These observations are in line with those reported by Vishali et al. [50]. The time for 50% breakthrough (τ) decreased at elevated flow rates because of the limited contact time between the contaminants and the bone char. In contrast to this, increments in bed height resulted in a decline in K_{YN} values and an increase in τ values. The rise in τ is due to the rise in residence time at increased bed heights. A similar report was also given by Saadi et al. [43]. The experimental data for COD and colour adsorption fitted well with the model, as shown in Figures 11(a), 11(b),12(a), and 12(b) with R^2 values ranging from 0.9037 to 0.9796. Additionally, the predicted and experimental τ values (Table 9) were in close alignment, confirming the suitability of the Yoon–Nelson model for the proposed fixed bed adsorption system. The aptness of the Yoon–Nelson model to the experimental data asserts that the rate of decrease in the adsorption reaction is reliant on the breakthrough and the adsorption of the adsorbate species on the adsorbent [52].

3.5. Comparison of Bone Char with Other Adsorbents. The adsorption capacities and efficiencies of different adsorbents in the removal of colour and COD from different studies are compared with the results obtained in this study in Table 10.

4. Conclusion

The applicability of bone char as a suitable adsorbent for efficient, simultaneous removal of organic substances and colour from real tannery wastewater was evaluated in this study. The effects of different operating conditions, including packed bed height and wastewater flow rate, on the efficiency of a fixed bed column were investigated through breakthrough curve analysis. Evidently, an increase in bed heights and a decrease in flow rates enhanced the adsorption efficiency of the bone char. The optimal process conditions achieved were 15 cm bed height and 2 mL/min flow rate. The maximum adsorption capacities and efficiencies attained at these optimal conditions were 227.4 mg/g and 80.65%, respectively, for COD and 53.03 Pt-Co/g and 84%, respectively, for colour. Fitting the experimental results to the Thomas, Adams–Bohart, and the Yoon–Nelson models revealed that the Yoon–Nelson model yielded the best prediction of the experimental results. From the findings of this study, it is evident that bone char is a highly potential low-cost, and an efficient green alternative for the treatment of tannery wastewater. It is, however, recommended that further studies should be carried out to ascertain the impact of the bone char characteristics on its adsorption efficiency and also to elucidate the effect of the presence of other contaminants on the adsorption capacity of the bone char.

Data Availability

All data supporting the findings of this research study are presented in this article.

Conflicts of Interest

The authors declare that they have no conflicts of interest.

Acknowledgments

This study was funded by the Regional Water and Environmental Sanitation Centre Kumasi (RWESCK) at the Kwame Nkrumah University of Science and Technology, Kumasi, with funding from the Ghana Government through the World Bank under the Africa Centres of Excellence project. The authors also thank Mr. Emmanuel Nketiah Ahenkorah for assisting in setting up the fixed bed columns.

References

[1] M. C. Liu, C.-M. Chen, H. Y. Cheng, H. Y. Chen, Y. C. Su, and T. Y. Hung, "Toxicity of different industrial effluents in Taiwan: a comparison of the sensitivity of *Daphnia similis* and Microtox®," *Environmental Toxicology*, vol. 17, no. 2, pp. 93–97, 2002.

[2] M. Appiah-Brempong, H. M. K. Essandoh, N. Y. Asiedu, S. K. Dadzie, and F. W. Y. Momade, "An insight into artisanal leather making in Ghana," *Journal of Leather Science and Engineering*, vol. 2, no. 1, pp. 1–14, 2020.

[3] S. Dixit, A. Yadav, P. D. Dwivedi, and M. Das, "Toxic hazards of leather industry and technologies to combat threat: a review," *Journal of Cleaner Production*, vol. 87, pp. 39–49, 2015.

[4] G. Durai and M. Rajasimman, "Biological treatment of tannery wastewater—a review," *Journal of Environmental Science and Technology*, vol. 4, no. 1, pp. 1–17, 2010.

[5] M. Appiah-Brempong, H. M. K. Essandoh, N. Y. Asiedu, S. K. Dadzie, and F. W. Y. Momade, "Artisanal tannery wastewater: quantity and characteristics," *Heliyon*, vol. 8, no. 1, Article ID e08680, 2022.

[6] P. K. Gosh and M. D. Hossain, "Assessment of tannery effluent: a case study of Dhaleshwari river in Bangladesh," in *Proceedings of International Conference on Planning, Architecture and Civil Engineering*, vol. 2, no. 7, pp. 461–464, 2019.

[7] E. Ifeanyi, V. Istifanus, and K. Z. Shehu, "Investigating the effect of tannery effluent discharge on groundwater quality in Challawa, Kano State, Nigeria," *International Journal of Scientific Research*, vol. 11, no. 1, pp. 1358–1362, 2022.

[8] H. R. Amanial, "Physico-chemical characterization of tannery effluent and its impact on the nearby river," *Journal of Environmental Chemistry and Ecotoxicology*, vol. 8, no. 6, pp. 44–50, 2016.

[9] M. Appiah-Brempong, H. M. K. Essandoh, N. Y. Asiedu, G. Ntoni, and F. Y. Momade, "Removal of colour and COD from vegetable tannery wastewater onto bone char—effect of process parameters, adsorption mechanism, kinetics and equilibrium modelling," *Separation Science and Technology*, pp. 1–20, 2023.

[10] M. Chowdhury, M. G. Mostafa, T. K. Biswas, and A. K. Saha, "Treatment of leather industrial effluents by filtration and coagulation processes," *Water Resources and Industry*, vol. 3, pp. 11–22, 2013.

[11] G. L. Tadesse, "Impacts of tannery effluent on environments and human health: a review article," *Advances in Life Science and Technology*, vol. 54, pp. 58–67, 2017.

[12] H. Q. Ali, M. U. Yasir, A. Farooq, M. Khan, M. Salman, and M. Waqar, "Tanneries impact on groundwater quality: a case study of Kasur city in Pakistan," *Environmental Monitoring and Assessment*, vol. 194, no. 11, pp. 1–15, 2022.

[13] UN and Sustainable Development Goal 6, "Sustainable development goal 6 synthesis report on water and sanitation," New York, USA, 2018.

[14] J. Zhao, Q. Wu, Y. Tang, J. Zhou, and H. Guo, "Tannery wastewater treatment: conventional and promising processes, an updated 20-year review," *Journal of Leather Science and Engineering*, vol. 4, no. 1, pp. 1–22, 2022.

[15] G. Crini and E. Lichtfouse, "Advantages and disadvantages of techniques used for wastewater treatment," *Environmental Chemistry Letters*, vol. 17, no. 1, pp. 145–155, 2019.

[16] A. K. Verma, R. R. Dash, and P. Bhunia, "A review on chemical coagulation/flocculation technologies for removal of colour from textile wastewaters," *Journal of Environmental Management*, vol. 93, no. 1, pp. 154–168, 2012.

[17] M. Appiah-Brempong, H. M. K. Essandoh, N. Asiedu, S. K. Dadzie, and F. Y. Momade, "Performance optimization of chemical and green coagulants in tannery wastewater treatment: a response surface methodology approach," *Journal of Optimization*, vol. 2023, Article ID 9939499, 19 pages, 2023.

[18] S. Kim, "Application of response surface method as an experimental design to optimize coagulation–flocculation process for pre-treating paper wastewater," *Journal of Industrial and Engineering Chemistry*, vol. 38, pp. 93–102, 2016.

[19] T. Ahmed, S. I. Promi, and I. J. Rumpa, "Colour removal of tannery wastewater using activated carbon generated from rice husk," in *World Environmental and Water Resources Congress 2018*, pp. 312–321, 2018.

[20] Q. He, K. Yao, D. Sun, and B. Shi, "Biodegradability of tannin-containing wastewater from leather industry," *Biodegradation*, vol. 18, no. 4, pp. 465–472, 2007.

[21] S. Afroze and T. K. Sen, "A review on heavy metal ions and dye adsorption from water by agricultural solid waste adsorbents," *Water, Air, & Soil Pollution*, vol. 229, no. 7, pp. 1–50, 2018.

[22] D. Lakherwal, "Adsorption of heavy metals: a review," *International Journal of Environmental Research and Development*, vol. 4, no. 1, pp. 2249–3131, 2014.

[23] L. W. Low, T. T. Teng, N. Morad, and B. Azahari, "Optimization of the column studies into the adsorption of basic dye using tartaric acid-treated bagasse," *Desalination and Water Treatment*, vol. 52, no. 31–33, pp. 6194–6205, 2014.

[24] G. Crini, E. Lichtfouse, L. D. Wilson, and N. Morin-Crini, "Conventional and non-conventional adsorbents for wastewater treatment," *Environmental Chemistry Letters*, vol. 17, no. 1, pp. 195–213, 2019.

[25] A. Rahaman, M. R. Hosen, M. A. Hena, U. H. B. Naher, and M. Moniruzzaman, "A study on removal of chromium from tannery effluent treatment of chrome tanning waste water using tannery solid waste," *International Journal and Human Capital in Urban Management*, vol. 1, no. 4, pp. 237–242, 2016.

[26] M. Nur-E-Alam, M. A. S. Mia, F. Ahmad, and M. M. Rahman, "An overview of chromium removal techniques from tannery effluent," *Applied Water Science*, vol. 10, no. 9, pp. 1–22, 2020.

[27] M. Fabbricino and R. Gallo, "Chromium removal from tannery wastewater using ground shrimp shells chromium removal from tannery wastewater using ground shrimp shells," *Desalination and Water Treatment*, vol. 23, pp. 1–5, 2020.

[28] T. Adane and A. Dessie, "Adaptability of Teff husk activated carbon for removal of hexavalent chromium from tannery wastewater at optimized process condition," *Applied Water Science*, vol. 10, no. 8, pp. 1–7, 2020.

[29] M. D. Islam, A. Rahaman, M. M. Mahdi, and D. Mallik, "Removal of Cr(III) and other pollutants from tannery wastewater by Moringa stenopetela seed," *IOP Conference Series: Earth and Environmental Science*, vol. 644, no. 1, Article ID 012025, 2021.

[30] S. M. Alam, Al-Mizan, M. Parvin, T. Uddin, M. Zahangir, and M. Alam, "Preparation of activated cow bone charcoal for abatement of water pollution caused by tannery effluents," *International Journal of Current Research*, vol. 10, no. 5, pp. 68929–68933, 2018.

[31] M. R. Hosen, A. Rahaman, M. A. Hena, M. M. Hasan, U. H. B. Naher, and M. Moniruzzaman, "Removal of chromium from tannery effluent using plant bark and leaf," *Energy and Environment Focus*, vol. 6, no. 2, pp. 139–144, 2017.

[32] D. H. Carrales-Alvarado, B. A. Jiménez-López, R. Leyva-Ramos et al., "Bone char modification by iron to improve its capacity for adsorbing fluoride from an aqueous solution," *Sustainable Environment Research*, vol. 33, no. 1, pp. 1–12, 2023.

[33] M. Saffari and M. Moazallahi, "Evaluation of slow-pyrolysis process effect on adsorption characteristics of cow bone for Ni ion removal from Ni-contaminated aqueous solutions," *Pollution*, vol. 8, no. 3, pp. 1076–1087, 2022.

[34] S. Dahbi, M. Azzi, M. Saib, L. M. de Guardia, R. Faure, and R. N. Durand, "Removal of trivalent chromium from tannery waste waters using bone charcoal," *Analytical and Bioanalytical Chemistry*, vol. 374, no. 3, pp. 540–546, 2002.

[35] P. Jia, H. Tan, K. Liu, and W. Gao, "Removal of methylene blue from aqueous solution by bone char," *Applied Sciences*, vol. 8, no. 10, Article ID 1903, 2018.

[36] C. Harripersadth and P. Musonge, "The dynamic behaviour of a binary adsorbent in a fixed bed column for the removal of Pb2+ Ions from contaminated water bodies," *Sustainability*, vol. 14, no. 13, Article ID 7662, 2022.

[37] H. D. S. S. Karunarathne and B. M. W. P. K. Amarasinghe, "Fixed bed adsorption column studies for the removal of aqueous phenol from activated carbon prepared from sugarcane bagasse," *Energy Procedia*, vol. 34, pp. 83–90, 2013.

[38] W. Tsai, M. D. G. de Luna, H. L. P. Bermillo-arriesgado, C. M. Futalan, J. I. Colades, and M.-W. Wan, "Competitive fixed-bed adsorption of Pb(II), Cu(II), and Ni(II) from aqueous solution using chitosan-coated bentonite," *International Journal of Polymer Science*, vol. 2016, Article ID 1608939, 11 pages, 2016.

[39] APHA, AWWA, and WPCF, *Standard Methods for the Examination of Water And Wastewater*, American Public Health Association, Washington, D.C., 20th edition, 1999.

[40] C. K. Rojas-Mayorga, D. I. Mendoza-Castillo, A. Bonilla-Petriciolet, and J. Silvestre-Albero, "Tailoring the adsorption behavior of bone char for heavy metal removal from aqueous solution," *Adsorption Science & Technology*, vol. 34, no. 6, pp. 368–387, 2016.

[41] Z. Z. Chowdhury, S. B. Abd Hamid, and S. M. Zain, "Evaluating design parameters for breakthrough curve analysis and kinetics of fixed bed columns for Cu(II) cations using lignocellulosic wastes," *Bioresources*, vol. 10, no. 1, pp. 732–749, 2015.

[42] S. Afroze, T. K. Sen, and H. M. Ang, "Adsorption performance of continuous fixed bed column for the removal of methylene blue (MB) dye using *Eucalyptus sheathiana* bark biomass," *Research on Chemical Intermediates*, vol. 42, no. 3, pp. 2343–2364, 2016.

[43] Z. Saadi, R. Saadi, and R. Fazaeli, "Fixed-bed adsorption dynamics of Pb (II) adsorption from aqueous solution using nanostructured γ-alumina," *Journal of Nanostructure in Chemistry*, vol. 3, no. 1, pp. 2–8, 2013.

[44] Ghana Environmental Protection Agency, *General Environmental Quality Standards (Ghana)*, Ghana Environmental Protection Agency, Kumasi, Ashanti Region, Ghana, 2016.

[45] J. Coates, "Interpretation of infrared spectra, a practical approach," *Encyclopedia of Analytical Chemistry*, vol. 1–23, 2006.

[46] C. K. Rojas-Mayorga, J. Silvestre-Albero, I. A. Aguayo-Villarreal, D. I. Mendoza-Castillo, and A. Bonilla-Petriciolet, "A new synthesis route for bone chars using CO_2 atmosphere and their application as fluoride adsorbents," *Microporous and Mesoporous Materials*, vol. 209, pp. 38–44, 2015.

[47] M. K. Shahid, J. Y. Kim, and Y.-G. Choi, "Synthesis of bone char from cattle bones and its application for fluoride removal from the contaminated water," *Groundwater for Sustainable Development*, vol. 8, pp. 324–331, 2019.

[48] M. Krzesińska and J. Majewska, "Physical properties of continuous matrix of porous natural hydroxyapatite related to the pyrolysis temperature of animal bones precursors," *Journal of Analytical and Applied Pyrolysis*, vol. 116, pp. 202–214, 2015.

[49] K. M. Yahuza, M. B. Ibrahim, A. M. Ayuba, and R. S. Hamza, "Fixed-bed column adsorption of methyl blue using carbon derived from axle-wood (*Anogeissus leiocarpus*) stem as adsorbent," *Bayero Journal of Pure and Applied Sciences*, vol. 10, no. 1, pp. 304–310, 2017.

[50] S. Vishali, P. Mullai, and R. Karthikeyan, "Breakthrough studies and mass transfer studies on the decolourization of paint industry wastewater using encapsulated beads of Cactus opuntia (*Ficus indica*)," *Desalination and Water Treatment*, vol. 1–13, 2020.

[51] M. A. Acheampong, K. Pakshirajan, A. P. Annachhatre, and P. N. L. Lens, "Removal of Cu(II) by biosorption onto coconut shell in fixed-bed column systems," *Journal of Industrial and Engineering Chemistry*, vol. 19, no. 3, pp. 841–848, 2013.

[52] H. Patel, "Fixed-bed column adsorption study: a comprehensive review," *Applied Water Science*, vol. 9, no. 3, pp. 1–17, 2019.

[53] J. López-Cervantes, D. I. Sánchez-Machado, R. G. Sánchez-Duarte, and M. A. Correa-Murrieta, "Study of a fixed-bed column in the adsorption of an azo dye from an aqueous medium using a chitosan–glutaraldehyde biosorbent," *Adsorption Science & Technology*, vol. 36, no. 1-2, pp. 215–232, 2018.

[54] Q. Hu, S. Pang, D. Wang, Y. Yang, and H. Liu, "Deeper insights into the Bohart–Adams model in a fixed-Bed column," *The Journal of Physical Chemistry B*, vol. 125, no. 30, pp. 8494–8501, 2021.

[55] A. S. Kovo, S. Alaya-Ibrahim, A. S. Abdulkareem et al., "Column adsorption of biological oxygen demand, chemical oxygen demand and total organic carbon from wastewater by magnetite nanoparticles-zeolite A composite," *Heliyon*, vol. 9, no. 2, Article ID e13095, 2023.

[56] A. A. Ahmad, A. Idris, and B. H. Hameed, "Color and COD reduction from cotton textile processing wastewater by activated carbon derived from solid waste in column mode," *Desalination and Water Treatment*, vol. 41, no. 1–3, pp. 224–231, 2012.

[57] M. Oteng-Peprah, P. A. Obeng, M. A. Acheampong, and M. A. Anang, "Fixed-bed column sorption kinetic rates on the removal of both biochemical oxygen demand (BOD5) and chemical oxygen demand (COD) in domestic greywater by using palm kernel activated carbon," *Water Practice & Technology*, vol. 18, no. 7, pp. 1628–1638, 2023.

[58] S. Syafalni, I. Abustan, I. Dahlan, C. K. Wah, and G. Umar, "Treatment of dye wastewater using granular activated carbon and zeolite filter," *Modern Applied Sciences*, vol. 6, no. 2, pp. 37–51, 2012.

[59] S. Nopkhuntod, S. Dararat, and J. Yimrattanabovorn, "Removal of reactive dyes from wastewater by shale," *Songklanakarin Journal of Science Technology*, vol. 34, no. 1, pp. 117–123, 2012.